

Single mutation at the intersubunit interface confers extra efficiency to Cu,Zn superoxide dismutase

Maria Elena Stroppolo^a, Alessandra Pesce^b, Mattia Falconi^a, Peter O'Neill^c,
Martino Bolognesi^b, Alessandro Desideri^{a,*}

^aINFM, Dipartimento di Biologia, Università di Roma, Tor Vergata, Via della Ricerca Scientifica snc, 00133 Rome, Italy

^bINFM, Dipartimento di Fisica and Centro Biotecnologie Avanzate, Università di Genova, Largo Giovanna Benzi, 16150 Genoa, Italy

^cRadiation and Genome Stability Unit, Medical Research Council, Harwell, Didcot, Oxon OX11 0RD, UK

Received 2 June 2000; revised 29 July 2000; accepted 10 August 2000

Edited by Richard Cogdell

Abstract The Val28→Gly single mutant at the subunit interface of Cu,Zn superoxide dismutase from *Photobacterium leiognathi* displays a k_{cat}/K_M value of $1.7 \times 10^{10} \text{ M}^{-1} \text{ s}^{-1}$, twice that of the native enzyme. Analysis of the three-dimensional structure indicates that the active site Cu,Zn center is not perturbed, slight structural deviations being only localized in proximity of the mutation site. The enzyme–substrate association rate, calculated by Brownian dynamics simulation, is identical for both enzymes, indicating that the higher catalytic efficiency of the Val28→Gly mutant is not due to a more favorable electrostatic potential distribution. This result demonstrates the occurrence of an intramolecular communication between the mutation site and the catalytic center, about 18 Å away and indicates a new strategy to encode extra efficiency within other members of this enzymatic family. © 2000 Federation of European Biochemical Societies. Published by Elsevier Science B.V. All rights reserved.

Key words: Superoxide dismutase; Intersubunit contact; Extra efficient enzyme; Dynamical property

1. Introduction

Cu,Zn superoxide dismutases (Cu,Zn SODs) are a class of metallo-enzymes which catalyze the dismutation of the superoxide radical into oxygen and hydrogen peroxide, providing the cell's initial defence against oxidative damage [1]. Under turnover conditions, the copper ion at the enzyme active site cycles between the Cu(II) and Cu(I) redox states, following successive encounters with the superoxide anion substrate. The intramolecular electron transfer between substrate and the active site copper, in Cu,Zn SOD, is considered as an instance of extreme efficiency, the second order catalytic rate for the enzymatic reaction being limited, practically, only by substrate diffusion. In this respect, it has been shown that steering of the negatively charged substrate to the active site is enhanced by an appropriate distribution of the electrostatic field on the enzyme surface, around the active site [2,3]. In eukaryotic Cu,Zn SODs, such a distribution is conserved over the different species [4], providing the condition for conservation of the second order substrate–enzyme association rate

constant k_1 and of the the second order catalytic rate constant k_{cat}/K_M ratio [5,6]. The role of the electrostatic field distribution in enhancing substrate diffusion, in the eukaryotic enzymes, has been proved by a series of experiments in which rational deletion or insertion of negatively or positively charged residues by site-directed mutagenesis yielded mutants having the second order catalytic rate constant higher than that found in the wild-type enzyme, at low ionic strength [7,8].

A similar electrostatic mechanism for the attraction of the substrate has been found also for prokaryotic Cu,Zn SODs [9,10] which, although maintaining the typical β -barrel fold in each subunit, adopt a different quaternary structure assembly when compared to the eukaryotic enzymes. Moreover, they display a different location for the so called 'electrostatic loop' [11–13]. Nevertheless, also for prokaryotic Cu,Zn SODs, rational single-site mutation of charged amino acid residues has brought to the isolation of mutants having a catalytic rate higher than the wild-type enzyme [14].

In the present communication, we show that the second order catalytic rate constant for the enzymatic reaction can also be increased without any perturbation of the enzyme electrostatics. A single site mutation, Val28→Gly, at the *Photobacterium leiognathi* Cu,Zn SOD subunit interface, yields an extra efficient enzyme, indicating that intramolecular communication occurs between the mutation site and the active site, i.e. between two regions which are about 18 Å apart. Inspection of the three-dimensional (3D) structure, determined by X-ray diffraction, does not show any macroscopic structural deviation of the active site structure and Cu,Zn coordination, when compared to the wild-type protein, suggesting that subtle differences, possibly related to modified enzyme dynamics, can regulate the active site reactivity. These results highlight mutation at the subunit interface residues as a new strategy for the study and control of the second order catalytic rate constant in Cu,Zn SODs.

2. Materials and methods

Single site mutant Val28→Gly of the recombinant Cu,Zn SOD from *P. leiognathi* (PSOD) was prepared in a two step PCR approach, according to Landt et al. [15]. The amplified DNA was restricted with *EcoRI* and *HindIII* and subsequently cloned into vector pEMBL18, previously digested with the same restriction enzymes. The expression plasmid obtained was inserted into the *Escherichia coli* strain DH5 α , as for wild-type PSOD. Recombinant clones were grown in standard LB medium containing AMP (70 mg/ml) for 6 h at 37°C. Then 0.25 mM of CuSO₄ and 80 μ M of ZnSO₄ were added, and the cells were left to grow for another 2 h. Proteins were extracted and purified as previously described [16]. Proteins were purified to 98%, as judged by

*Corresponding author. Fax: (39)-06-7259 4326.

E-mail: desideri@uniroma2.it

Abbreviations: Cu,Zn SOD, Cu,Zn superoxide dismutase; PSOD, Cu,Zn superoxide dismutase from *Photobacterium leiognathi*

SDS-PAGE. Protein concentration was determined by the Lowry method [17]. Copper content of the protein samples was determined by EPR spectroscopy using a Cu^{2+} -EDTA solution as a standard.

Activity assays were carried out by the pulse radiolysis method based on the dependence of the first order rate of loss of O_2^- , monitored spectrophotometrically at 250 nm [18]. The enzyme was assayed in Tris-Mops buffer in the pH range 7.4–9.0, and in borate from pH 9 and above [9]. In all cases, the assay mixture contained 0.1 M ethanol and 0.1 mM EDTA and the buffer concentrations were varied between 0.01 and 0.03 M in order to keep the ionic strength constant to $I = 0.02$ M. The activity assays were carried out with $[\text{O}_2^-] \gg [\text{SOD}]$, i.e. under turn-over conditions. The reaction of superoxide with hydrogen dioxide is taken into account in the determination of the second order rate constant for interaction of superoxide with PSOD that was determined from measurements of the first order rate of loss of superoxide at three different enzyme concentrations (0.25, 0.50, 0.75 μM). The error of first order rate constant at a given enzyme concentration is at the most $\pm 10\%$. The enzyme concentration used was changed within the range stated in order to compensate for the lower activity at higher pH values [9]. By using fast protein liquid chromatography (FPLC), featured by Superdex 75 (Pharmacia), no changes in dimer–monomer equilibrium between the wild-type and the mutated enzyme were detected in function of concentration. Until 0.5 μM of protein concentration, the resolution limit of the FPLC UV recorder, both enzymes eluted as dimers (data not shown).

Brownian dynamics simulations of the diffusion of superoxide anion toward the active site under the influence of the protein-generated electrostatic field were carried out as previously described [6]. Electrostatic potential was calculated with the program DelPhi (Biosym, Inc.) using the focusing procedure [19]. Trajectories (10 000) were run for each simulation; values of 4 and 78.5 have been assigned to the dielectric constant of protein interior and solvent, respectively [20]. The ion exclusion radius was set to 2 Å. 3D coordinates of wild-type and Val28 \rightarrow Gly PSOD structure were used to simulate the enzyme substrate encounter.

Crystals of the mutant PSOD were grown under the same physico-chemical conditions previously described for the wild-type enzyme [11], at pH 4.5, from 20% PEG 8000, 0.1 M sodium chloride and 0.05 M sodium acetate solutions; they are isomorphous with those of the wild-type protein (space group R32, $a = b = 86.9$ Å, $c = 99.0$ Å, $\gamma = 120^\circ$). X-ray diffraction data were collected at the EMBL-Hamburg synchrotron radiation facility ($\lambda = 0.84$ Å), at 100 K. The crystallization mother liquor was modified to 30% PEG 8000, 0.1 M sodium chloride, 0.05 M sodium acetate, 10% glycerol, for cryo-protection. Diffraction data were collected at 2.2 Å resolution and processed using DENZO [21]; see Table 1) and programs from the CCP4 suite [22]. Refinement of the Val28 \rightarrow Gly mutant 3D structure was achieved using the program REFMAC [23]; inspection of models and maps throughout the refinement was based on the O package [24]. The refined model displays stereochemical parameters close to ideality [25] and contains 57 water molecules. The final R -factor value is 21.1% (R -free 30.6%) for all the data in the 24.5–2.2 Å resolution range (see Table 1). Structure solution and refinement of the wild-type PSOD have been described previously (R -factor = 19.1%, at 2.1 Å resolution; data at 100 K; [11]).

3. Results and discussion

We engineered the Val28 \rightarrow Gly mutation in *P. leiognathi* Cu,Zn SOD; residue Val28 is involved in building the inter-subunit contacts in the homodimeric wild-type enzyme, and is located ca. 18 Å away from the active site, within its own subunit. The replacement of Val28 residue with Gly affects the 3D structure of the mutant enzyme to a minor extent, as evidenced by the 0.27 Å rms deviation measured between the C α atoms of the wild-type and mutant proteins (calculated over 139 C α atoms of one Cu,Zn SOD subunit, excluding 1–6 and 146–151 C α atoms, belonging to the mobile chain extremities). Comparison of the wild-type and Val28 \rightarrow Gly mutant crystal structures indicates evident structural variations, essentially localized in the proximity of the mutation site. In particular, the side chains of Asn23, Lys24, Met40, Leu85,

Asn95, Pro96 and Pro100, located at the subunit interface, are affected by the loss of Val28 aliphatic residue (see Fig. 1). Nevertheless, with the exception of the loss of van der Waals contacts between Val28 and Trp73, most of the inter-subunit contacts observed in the wild-type enzyme structure are conserved in the Val28 \rightarrow Gly mutant. A new intersubunit contact site is observed at residues Met40/Asn95', while the Tyr25/Pro100' contact is lost in the mutant enzyme. The general conservation of interface contacts extends to the structural cluster of water molecules mediating subunit interactions in the wild-type enzyme, in agreement with the neutral nature of the replaced residue at site 28 [11].

Within experimental error, the active site Cu,Zn center coordination geometry is unperturbed by the Val28 \rightarrow Gly mutation, the copper coordination distances being closely comparable with those found in the wild-type enzyme structure [11]. Close inspection of the Val28 \rightarrow Gly mutant structure indicates that the interface residue mutation may slightly affect the enzyme quaternary structure. Optimal superposition of subunit A of the Val28 \rightarrow Gly mutant structure with subunit A of the wild-type enzyme produces slightly different locations for the respective B subunits of the dimeric enzyme. As a general trend, possibly related to the presence of a smaller interface residue at site 28, in the Val28 \rightarrow Gly mutant dimer, the two subunits appear closer to each other (by ca. 0.5 Å) than in the wild-type enzyme structure. For example, the distance between the two active site Cu ions is 32.0 Å in the mutant and 32.7 Å in the wild-type enzyme.

The pH dependence of the second order catalytic rate constant displayed by the Val28 \rightarrow Gly mutant is shown in Fig. 2, in comparison with that of the wild-type protein; the pH dependence is similar for both enzymes. However, the rate constant for the mutant Cu,Zn SOD is twice as high as that of the wild-type enzyme in the pH range 7–9, but decreases to com-

Table 1
X-ray data collection and refinement statistics

<i>Data collection</i>	
Reflections measured	73 400
Resolution range (Å)	24.5–2.2
Independent reflections	7 022
$I/\sigma(I)$	20
R -merge	4.4%
Completeness	94.7%
Space group	R32
Unit cell	$a = b = 86.0$ Å, $c = 98.6$ Å, $\gamma = 120^\circ$
<i>Refinement</i>	
Refinement resolution range (Å)	24.5–2.2
Reflections used in refinement	6 283
Protein atoms	1 035
Cu,Zn atoms	2
Water molecules	57
R -factor/ R -free ^a	0.211/0.306
B -factor protein (Å ²)	35
B -factor solvent (Å ²)	35
B -factor Cu,Zn (Å ²)	29
Rmsd from ideal values:	
bond lengths (Å)	0.010
bond angles (Å)	0.035
Ramachandran plot ^b :	
Residues in most favored regions	82.3%
Residues in additional allowed regions	17.7%

^aCalculated using 10% of the reflections.

^bData produced using the program PROCHECK [29].

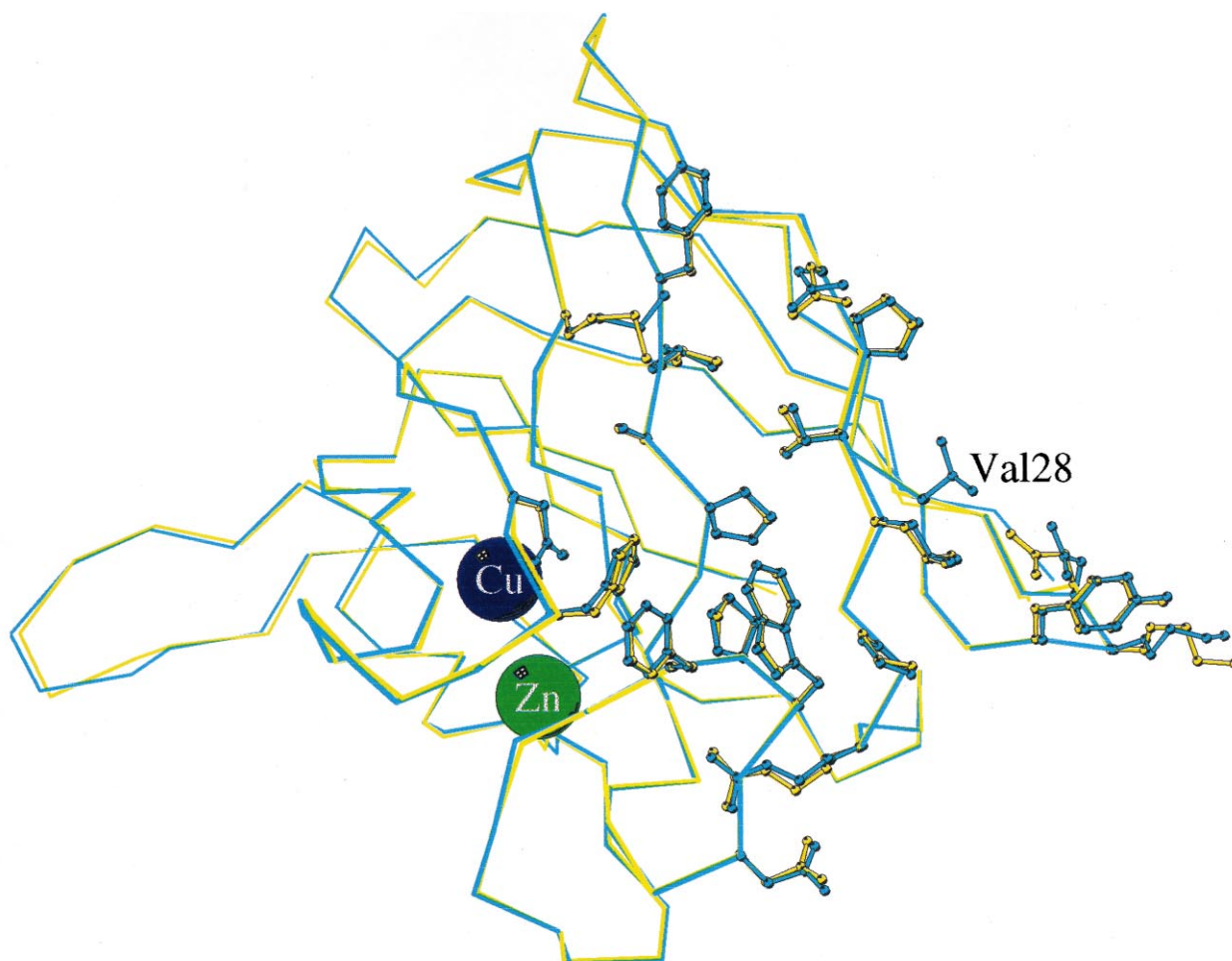


Fig. 1. Chain trace of the Val29→Gly A subunit (yellow), superimposed to the chain trace of wild-type A subunit (cyan). The ball and stick side-chains show the positions of the interface residues from the inter-subunit surface point of view. The blue and green spheres represent the copper and zinc ions, respectively. This picture was produced by using the MolScript v1.4 program [30].

parable values above pH 10, indicating that titration of the positively charged amino acids strongly reduces in both enzymes the superoxide attraction [9]. At neutral pH, the mutant SOD displays a $k_{\text{cat}}/K_{\text{M}}$ value of $1.7 \times 10^{10} \text{ M}^{-1} \text{ s}^{-1}$, i.e. the mutant enzyme is the most efficient Cu,Zn SOD so far reported.

Brownian dynamics simulation [6] based on the atomic coordinates of the independently determined X-ray crystal structures of the wild-type and Val28→Gly Cu,Zn SODs yields identical enzyme–substrate association rate values for both the native and the mutated enzyme. Such an observation indicates that the enhanced catalytic rate should not result from a more favorable electrostatic potential distribution, as observed in previously reported mutant forms [7,8,14]. Rather, the different catalytic efficiencies of the wild-type and mutated enzyme are to be ascribed to more subtle changes, that allow long range communication between the subunit interface and the active site. In this respect, we note that PSOD residues 26–46 (β -strand 3c, 3,6 loop and β -strand 6d) are involved in structural assembly of the active site, together with the S-S subloop (residues 46–55). Due to its critical location within the protein, the 26–46 region is a potential candidate for transducing towards the active site region structural and dynamic perturbations occurring at the subunit interface, at and

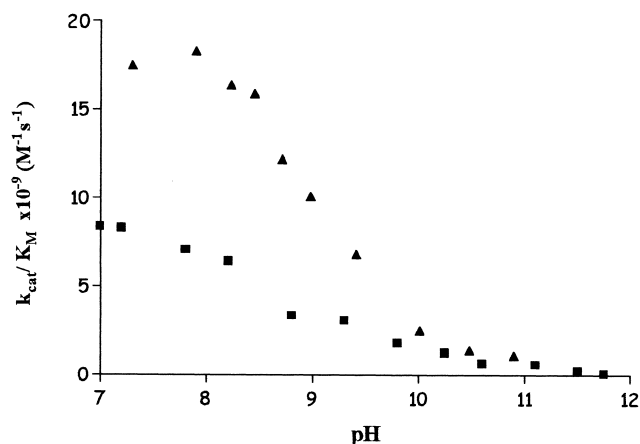


Fig. 2. Effect of pH on the catalytic rate constant ($k_{\text{cat}}/K_{\text{M}}$) for wild-type (■) and Val29→Gly (▲) mutant enzyme, determined by pulse radiolysis. The assays for both enzymes were carried out at 20°C and 20 mM ionic strength. The protein concentration for each sample varied in the range 0.25–0.75 μM .

around Val28 or Gly28, in the wild-type and mutated enzymes, respectively. Similarly, the structural and dynamical behavior of the S–S subloop may echo in the active site region differences in contacts/flexibility encoded at the enzyme subunit interface by residue mutations.

The experimental resolution of the X-ray diffraction data does not permit detection of significant changes in the active site structure, nor does it allow accurate enough refinement of the crystallographic *B*-factors to determine specific dynamic differences between the wild-type and the mutated proteins. However, previous molecular dynamics simulation studies on Cu,Zn SODs have proposed a fast inter-subunit communication correlated with motions of the loops surrounding the active site [26]. Moreover, recent X-ray diffraction studies on yeast and ox Cu,Zn SODs have shown that intermolecular crystal contacts can affect the enzyme active site through modulation of the Cu(II) redox potential, suggesting a subtle correlation between the active site properties and structural features located at the enzyme surface. Accordingly, very recently, it has been demonstrated that in PSOD mutants, whose residue Trp73 has been selectively mutated to Phe or Tyr, removal and addition of Zn(II) induces monomerization and dimerization of the enzyme, respectively, providing an unambiguous proof of direct communication between the subunit interface and the active site metals center [27]. The long range role of the subunit interface in affecting enzymatic activity is further stressed by evidence that the engineered monomeric human Cu,Zn SOD, mutated at the interface, displays activities much lower than that of the native enzyme [28]. In the case of PSOD Val28→Gly mutant, here presented, we show that mutation of a residue involved in subunit association affects the active site positively, yielding a very efficient mutant Cu,Zn SOD with a k_{cat}/K_M value twice that of the wild-type enzyme. We propose intersubunit mutation to be considered as a new strategy to confer extra efficiency to Cu,Zn SODs.

References

- [1] Bannister, J.V., Bannister, W.H. and Rotilio, G. (1987) *CRC Crit. Rev. Biochem.* 22, 111–180.
- [2] Koppenol, W.H. (1981) *The Physiological Role of The Charge Distribution on Superoxide Dismutase. Oxygen and Oxy-radicals in Chemistry and Biology* (Rodger, M.A.J. and Powers, E.L., Eds.), pp. 671–674, Academic Press, New York.
- [3] Getzoff, E., Tainer, J.A., Weiner, P.K., Kollman, P.A., Richardson, J.S. and Richardson, D.C. (1983) *Nature* 306, 287–290.
- [4] Desideri, A., Falconi, M., Polticelli, F., Bolognesi, M., Djinnovich, K. and Rotilio, G. (1992) *J. Mol. Biol.* 223, 337–342.
- [5] O'Neill, P., Davies, S., Calabrese, L., Capo, C., Marmocchi, F., Natoli, G. and Rotilio, G. (1988) *Biochem. J.* 251, 41–46.
- [6] Sergi, A., Ferrario, M., Polticelli, F., O'Neill, P. and Desideri, A. (1994) *J. Phys. Chem.* 98, 10554.
- [7] Getzoff, E.D., Cabelli, D.E., Fisher, C.L., Parge, H.E., Viezzoli, M.S., Banci, L. and Hallewell, R.A. (1992) *Nature* 358, 347–351.
- [8] Polticelli, F., Bottaro, G., Battistoni, A., Carri, M.T., Djinnovich-Carugo, K., Bolognesi, M., O'Neill, P., Rotilio, G. and Desideri, A. (1995) *Biochemistry* 34, 6043–6049.
- [9] Stroppolo, M.E., Sette, M., O'Neill, P., Polizio, F., Cambria, M.T. and Desideri, A. (1998) *Biochemistry* 37, 12287–12292.
- [10] Folcarelli, S., Battistoni, A., Falconi, M., O'Neill, P., Rotilio, G. and Desideri, A. (1998) *Biochem. Biophys. Res. Commun.* 244, 908–911.
- [11] Bordo, D., Matak, D., Djinnovich-Carugo, K., Rosano, C., Pesce, A., Bolognesi, M., Stroppolo, M.E., Falconi, M., Battistoni, A. and Desideri, A. (1999) *J. Mol. Biol.* 285, 283–296.
- [12] Bourne, J., Redford, S.M., Steinman, H.M., Lepock, J.R. and Tainer, J.A. (1996) *Proc. Natl. Acad. Sci. USA* 93, 12774–12779.
- [13] Pesce, A., Capasso, C., Battistoni, A., Folcarelli, S., Rotilio, G., Desideri, A. and Bolognesi, M. (1997) *J. Mol. Biol.* 274, 408–420.
- [14] Folcarelli, S., Venerini, F., Battistoni, A., O'Neill, P., Rotilio, G. and Desideri, A. (1999) *Biochem. Biophys. Res. Commun.* 256, 425–428.
- [15] Landt, O., Grunert, H.P. and Hahn, U. (1990) *Gene* 96, 125–128.
- [16] Foti, D., Lo Curto, B., Cuzzocrea, G., Stroppolo, M.E., Polizio, F., Venanzi, M. and Desideri, A. (1997) *Biochemistry* 36, 7109–7113.
- [17] Lowry, O.H., Rosebrough, N.J., Farr, A.R. and Randall, R.J. (1951) *J. Biol. Chem.* 193, 265–275.
- [18] Fielden, E.M., Roberts, P.B., Bray, R., Lowe, D., Mautner, G., Rotilio, G. and Calabrese, L. (1974) *Biochem. J.* 139, 49.
- [19] Gilson, M., Sharp, K.A. and Honig, B.H. (1987) *J. Comput. Chem.* 9, 327–335.
- [20] Gilson, M. and Honig, B. (1988) *Proteins* 4, 7–18.
- [21] Otwinowski, Z. and Minor, W. (1997) *Methods Enzymol.* 276, 307–326.
- [22] Collaborative Computational Project Number 4 (1994) *Acta Crystallogr.* D50, 760–763.
- [23] Murshudov, G.N., Vagin, A.A. and Dodson, E.J. (1997) *Acta Crystallogr.* D53, 240–255.
- [24] Jones, T.A., Cowan, S.W. and Kjeldgaard, M. (1991) *Acta Crystallogr.* A47, 110–119.
- [25] Engh, R.A. and Huber, R. (1991) *Acta Crystallogr.* A47, 392–400.
- [26] Chillemi, G., Falconi, M., Amadei, A., Zimatore, G., Desideri, A. and Di Nola, A. (1997) *Biophys. J.* 73, 1007–1018.
- [27] D'Orazio, M., Battistoni, A., Stroppolo, M.E. and Desideri, A. (2000) *Biochem. Biophys. Res. Commun.* (in press).
- [28] Banci, L., Benedetto, M., Bertini, I., Del Conte, R., Piccioli, M. and Viezzoli, M.S. (1998) *Biochemistry* 37, 11780–11791.
- [29] Laskowski, R.A., MacArthur, M.W., Moss, D.S. and Thornton, J.M. (1993) *J. Appl. Crystallogr.* A 47, 283–291.
- [30] Kraulis, P.J. (1991) *J. Appl. Crystallogr.* 24, 946–950.